IONOSPHERIC PROFILES FROM FAR ULTRAVIOLET REMOTE SENSING:

THE FORWARD MODEL

A. TAN

PRINCIPAL INVESTIGATOR
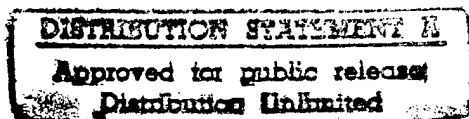
ANNUAL REPORT OF ONR GRANT NOOO14-97-1-0267

RESEARCH REPORT NO. AAMU-ONR-97-1

ALABAMA A&M UNIVERSITY

NORMAL, AL 35762

OCTOBER 1997

DTIC QUALITY INSPECTED 4

19971007 239

Ultraviolet remote sensing of the ionosphere

The goal of this project is to faithfully reconstruct ionospheric profiles from O^+-e^- recombination emissions in the far ultraviolet region of the electromagnetic spectrum as observed from polar orbitting space platforms.

The nighttime ionsophere

Remote sensing of the nighttime ionosphere is a more straightforward process because of the absence of the complications brought about by daytime solar ultraviolet radiation. This, therefore marks the starting point of the present investigation.

The midlatitude ionosphere

In the course of one revolution, a satellite in a sun-synchronous polar orbit encounters the equatorial and polar ionospheres twice each, but the midlatitude ionosphere four times. Remote sensing of the polar ionosphere is complicated by the presence of auroras. The equatorial ionosphere, on the other hand, possesses Appleton's anomaly, which also affects faithful reconstruction of its profile. The midlatitude ionosphere is relatively better stratified for the purpose of remote sensing.

The forward model

We first calculate the expected emission intensities from the O^+-e^- recombination as seen from an orbitting platform in a circular orbit using the forward model. The variation of the emission intensity with the observation angle is obtained from model ionospheric layers.

The Chapman layer

The standard 3-parameter Chapman layer electron density N as a function of the altitude z is given by

$$N(z) = N_m \, e^{\frac{1}{2} \left(1 - \frac{z - z_m}{H} - e^{-\frac{z - z_m}{H}} \right)} \qquad (1)$$

where N_m = peak electron density,

z_m = altitude of the peak,

and   H = scale height of O.

A parametric study of the expected emission intensities in N_m, z_m and H as seen from a fixed altitude in space is obtained.

The path matrix

Given the fixed altitude of the orbitting satellite, the path lengths through given stratified layers up to the satellite are calculated for different observation angles. The number of layers is rendered equal to the number of observation angles and a square path matrix is obtained for the purpose of subsequent inversion.

The inverse matrix

A matrix inversion program in double precision BASIC has been incorporated. It has successfully inverted path matrices of dimensions up to at least 29 x29.

The reconstructed profile

Standard model Chapman profiles have been reconstructed using the inverse path matrix. The reconstructed profile is accurate up to an altitude of about 1000 km. The errors above 1000 km are almost certainly due to the limits of computational accuracy.

Exponential and power altitude levels

The use of exponentially increasing layer heights has resulted in improved accuracy of the reconstructed profile at higher altitudes. Other power levels, such as, $z = 2^x$, 3^x, etc., have been tried. The best results were obtained by $z = 1.8^x$ for a standard Chapman layer up to about 1000 km for a 29 x 29 matrix.

Results of the forward model

The nighttime intensity of the radiative recombination of O^+-e^- at 91.1 nm as observed from the ARGOS satellite (altitude 833 km) is calculated. The reaction rate is assumed to be 4.4 x 10$^-$ [13] cm³/s (Dymond, et al., 1995). The standard Chapman profile is given by Eq. (1) with N_m =

10^6 cm^{-3}, z_m = 350 km and H = 60 km. Parametric study of the intensity of radiation in z_m, H and N_m are obtained and shown in Figs. (1), (2) and (3) respectively for nadir angles (complement of observation angle) between 66 deg and 73 deg.

Figure 1 shows that the peak intensity nadir angle translates about 1.1 deg for every 50 km increase of z_m. There is a slight but perceptible increase in the peak intensity with z_m.

Figure 2 shows the dependence of the intensity of radiation on H. The peak migrates to lower nadir angles with increase of H.

Figure 3 shows the dependence of the intensity on N_m. As expected, the former is proportional to the square of the latter.

The midlatitude nighttime H$^+$ density profile

Typical midlatitude O$^+$ and H$^+$ density profiles can be found in a paper by Hagen and Hsu (1974). A detailed numerical model of O$^+$ and H$^+$ by Tan and Wu (1981) closely reproduced the observations of Hagen and Hsu (1974). The nighttime O$^+$ density profile is well represented by a Chapman distribution of Eq. (1) with N_m = 2 x 10^5 cm^{-3}, z_m = 350 km and H = 50 km.

The nighttime H$^+$ density profile could not be fitted with a standard Chapman distribution. However, a reasonable fit was obtained by a modified Chapman distribution (henceforth referred to as Parabolic-Chapman profile) given by

$$N(z) = N_m \left(\frac{z}{z_m} \right)^2 e^{\frac{1}{2} \left(1 - \frac{z - z_m}{H} - e^{-\frac{z - z_m}{H}} \right)} \qquad (2)$$

with N_m = 10^4 cm^{-3}, z_m = 750 km and H = 170 km.

Figure 4 shows the observed, calculated and model H$^+$ density profiles for nighttime midlatitude locations. Clearly, the standard Chapman profile could not reproduce the bottomside H$^+$ densities, but the Parabolic-Chapman profile gave a fair representation of the H$^+$ densities.

The forward model with O$^+$ and H$^+$

The 91.1 nm emission intensity of O$^+$-e$^-$ recombination reaction for the midlatitude nighttime profiles given above is calculated with and without H$^+$ density.

Figure 5 shows that the contribution from H^+ is not very important for nadir angles between 66 deg and 73 deg. The difference becomes important at higher nadir angles as is revealed by Fig.6.

Current and future study

Currently, we are attempting to extend the accuracy of inversion from 1000 km to 1500 km. This will be followed by the actual task of reconstructing the O^+ and H^+ profiles from the remote sensing of the topside ionosphere.

References

Dymond, K. F., Thonnard, S. E. and McCoy, R. P., 1996 I. E. S., Alexandria, VA, May 1996.

Hagen, J. B. and Hsu, P. Y. S., J. Geophys. Res., 79, 4269 (1974).

Tan, A. and Wu, S. T., Geofis. Intl., 20, 11 (1981).

Fig. 1. Expected intensity of O^+-e^- recombination at 91.1 nm as observed from 833 km altitude for different z_m ($N_m = 10^6$ cm^{-3}; $H = 60$ km)
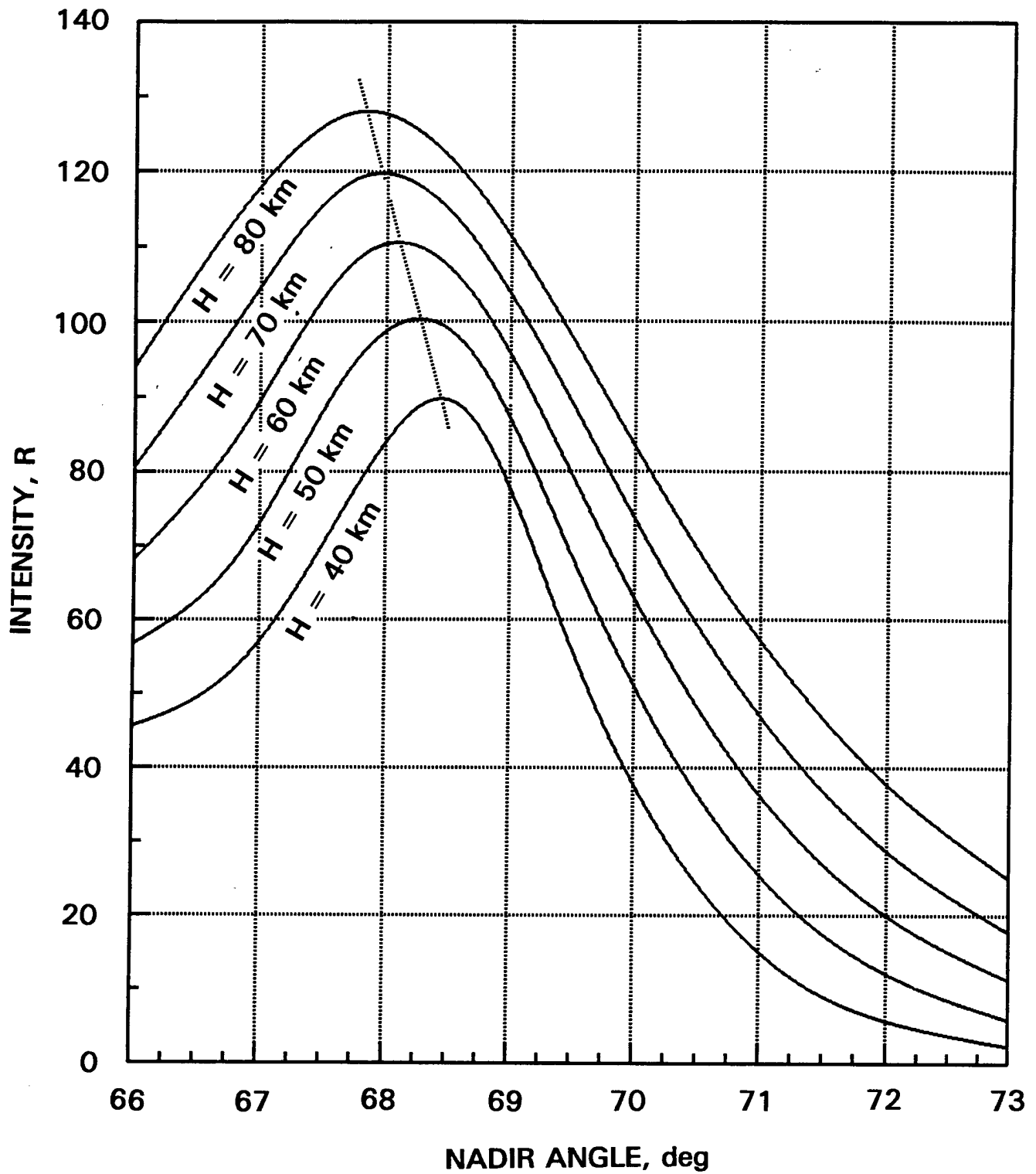
Fig. 2. Expected intensity of O^+-e^- recombination at 91.1 nm as observed from 833 km altitude for different H ($N_m = 10^6$ cm^{-3}; $z_m = 350$ km)

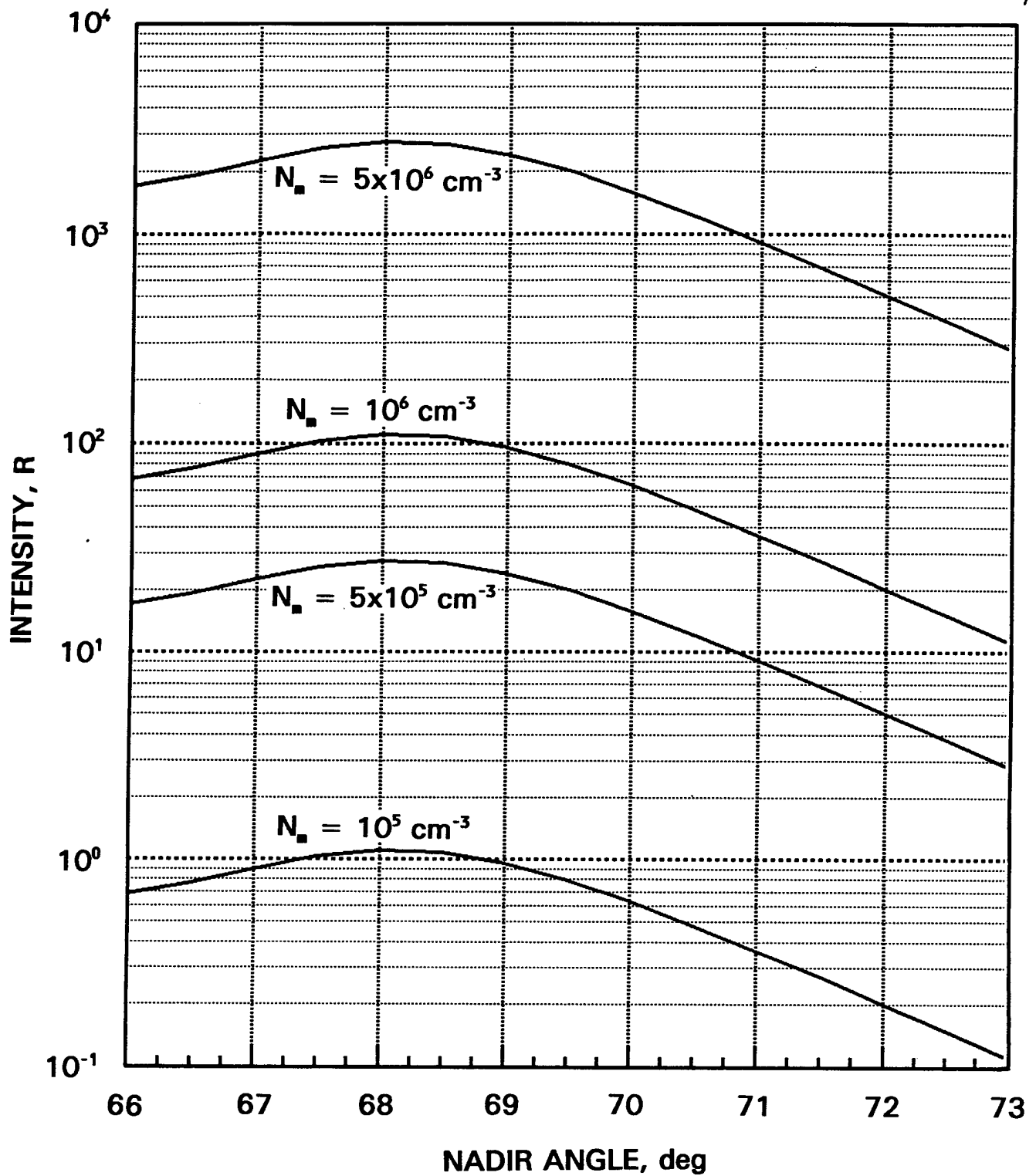Fig. 3. Expected intensity of O^+-e^- recombination at 91.1 nm as observed from 833 km altitude for different N_m ($z_m = 350$ km; $H = 60$ km)
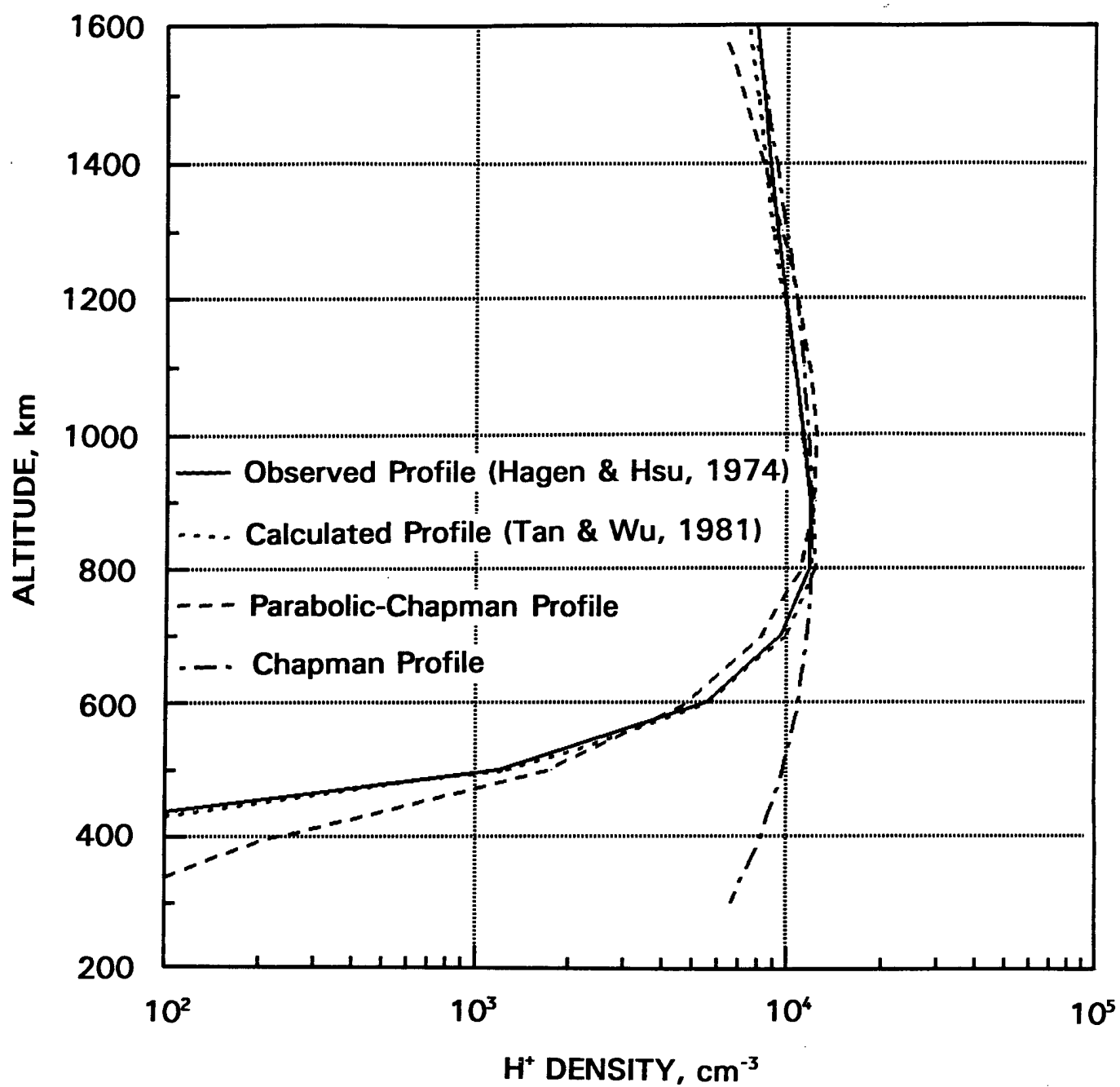
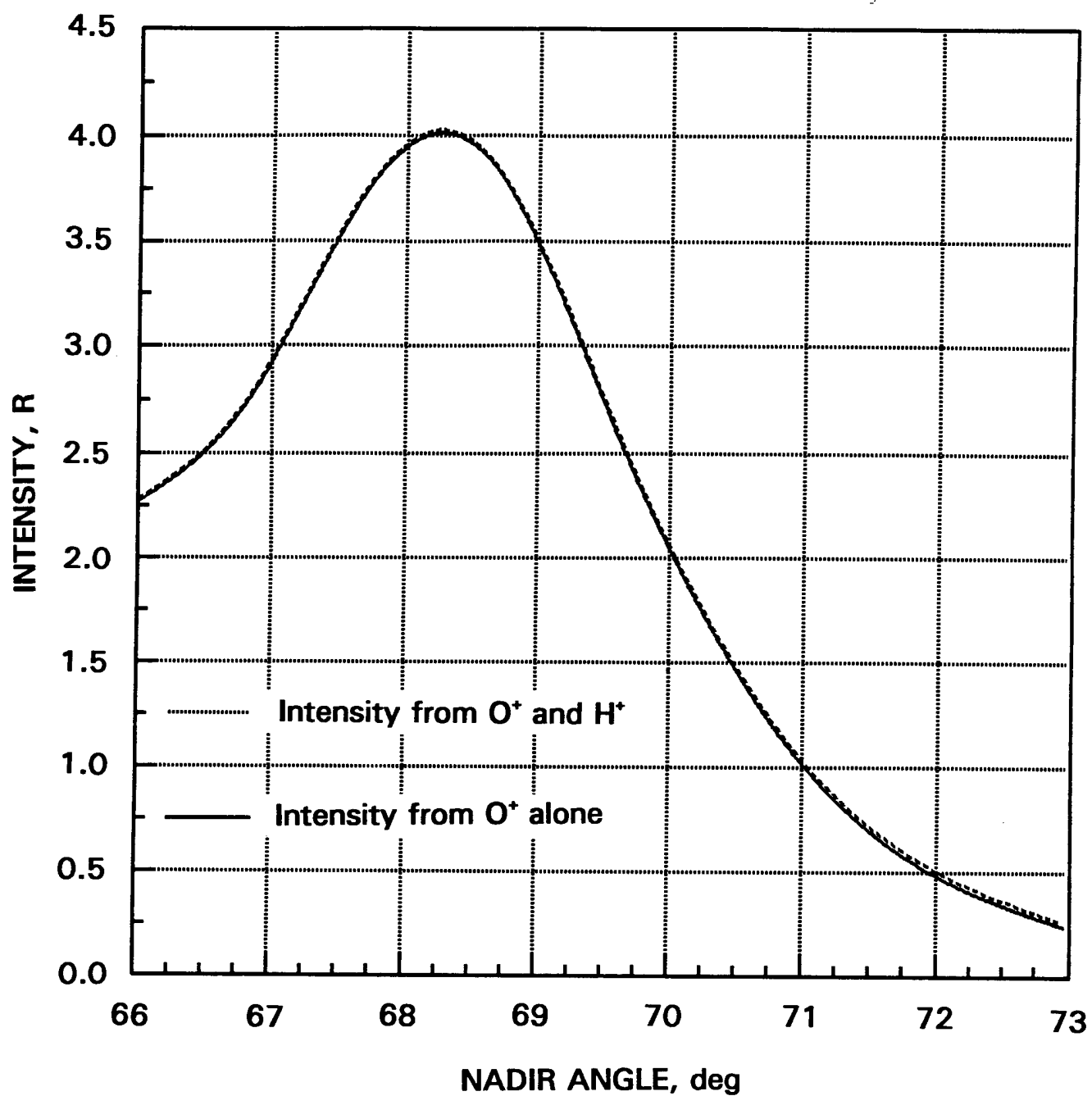Fig. 4. Representative profiles of nightime midlatitude H$^+$ density

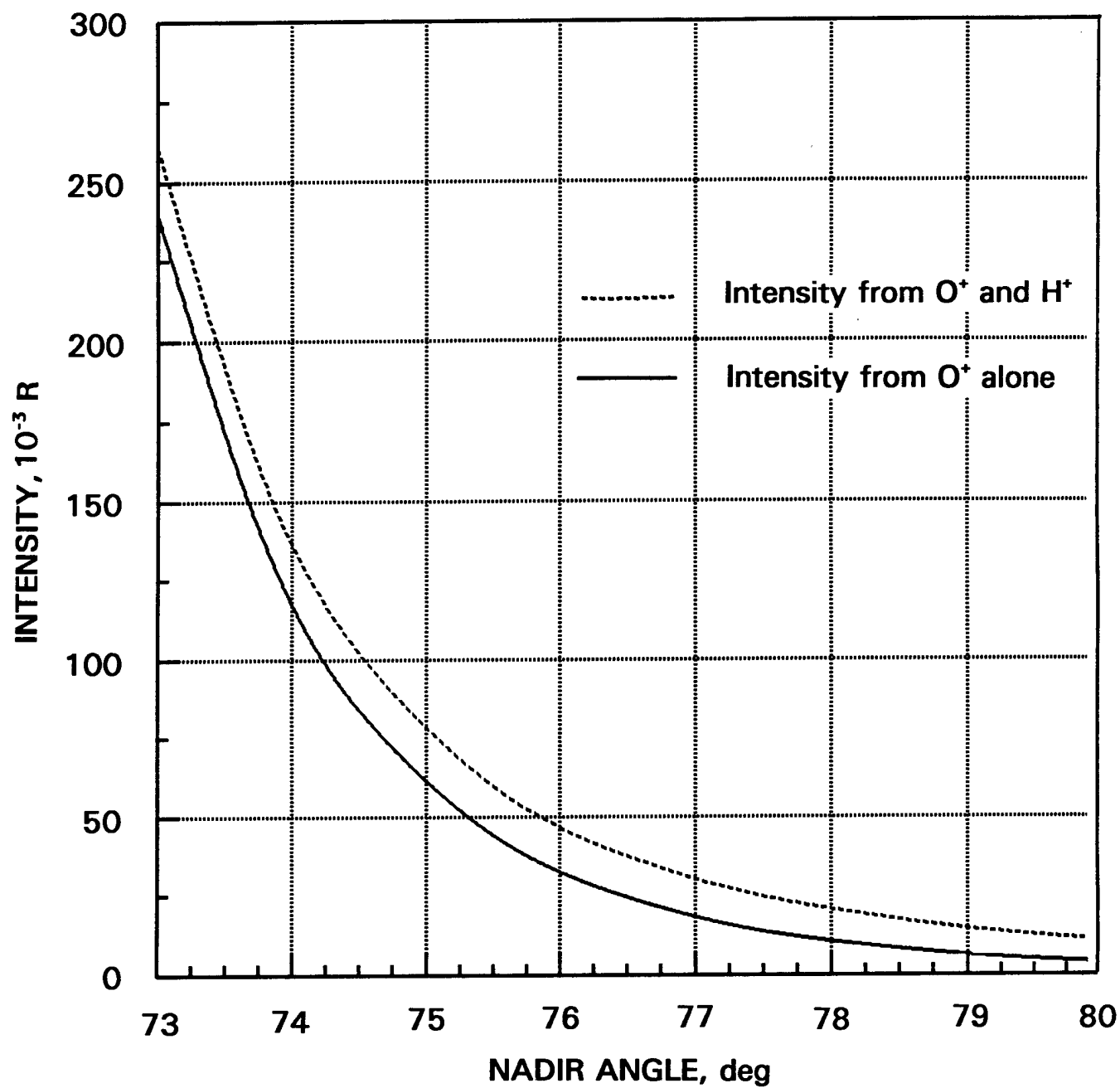Fig. 5. Expected intensity of O^+-e^- recombination at 91.1 nm as observed from 833 km altitude for nightime midlatitude locations with and without H^+ density

Fig. 6. Fig. 5 continued to higher nadir angles